

Lifetime of Almost Strong Edge-Mode Operators in One-Dimensional, Interacting, Symmetry Protected Topological Phases

Daniel J. Yates,¹ Alexander G. Abanov,^{2,3} and Aditi Mitra¹

¹*Center for Quantum Phenomena, Department of Physics, New York University,
726 Broadway, New York, New York 10003, USA*

²*Simons Center for Geometry and Physics, Stony Brook, New York 11794, USA*

³*Department of Physics and Astronomy, Stony Brook University, Stony Brook, New York 11794, USA*

 (Received 31 January 2020; revised manuscript received 27 April 2020; accepted 29 April 2020; published 22 May 2020)

Almost strong edge-mode operators arising at the boundaries of certain interacting one-dimensional symmetry protected topological phases with Z_2 symmetry have infinite temperature lifetimes that are nonperturbatively long in the integrability breaking terms, making them promising as bits for quantum information processing. We extract the lifetime of these edge-mode operators for small system sizes as well as in the thermodynamic limit. For the latter, a Lanczos scheme is employed to map the operator dynamics to a one-dimensional tight-binding model of a single particle in Krylov space. We find this model to be that of a spatially inhomogeneous Su-Schrieffer-Heeger model with a hopping amplitude that increases away from the boundary, and a dimerization that decreases away from the boundary. We associate this dimerized or staggered structure with the existence of the almost strong mode. Thus, the short time dynamics of the almost strong mode is that of the edge mode of the Su-Schrieffer-Heeger model, while the long time dynamics involves decay due to tunneling out of that mode, followed by chaotic operator spreading. We also show that competing scattering processes can lead to interference effects that can significantly enhance the lifetime.

DOI: [10.1103/PhysRevLett.124.206803](https://doi.org/10.1103/PhysRevLett.124.206803)

Topological states of matter are characterized by a bulk-boundary correspondence where nontrivial topological phases host robust edge modes [1–3]. While topological phases have been fully classified for free fermions [4], the stability of these phases to perturbations such as nonzero temperature, disorder, and interactions is poorly understood. The expectation is that, as long as the perturbations are smaller than the bulk single-particle energy gap, the edge modes will survive. More surprisingly, examples are beginning to emerge where, even at high temperatures of the order of the bandwidth and with moderate interactions, the edge modes, while not completely stable, have extremely long lifetimes [5–8]. Since edge modes can be used as qubits, understanding these nonperturbatively long lifetimes is of fundamental importance both for theory and for applications.

We study a class of one-dimensional models that in the limit of free fermions correspond to class D in the Altland-Zirnbauer classification scheme [4,9]. These models host Majorana modes and are promising candidates for non-Abelian quantum computing [10–16]. Adding interactions and raising the temperature do not appear to destabilize the edge modes easily [5–7,17,18]. Similar behavior has been found in interacting, disorder-free, Floquet systems where bulk quantities heat to infinite temperature rapidly, i.e., within a few drive cycles, and yet edge modes coexist with the high temperature bulk for an unusually long time [19]. A hurdle to understanding these lifetimes is that they are

extracted from exact diagonalization (ED), and this is plagued by system size effects, making it difficult to extract lifetimes in the thermodynamic limit.

We present a fundamentally new scheme to extract the long lifetimes of topological edge modes. Using a Lanczos scheme, we map the Heisenberg time evolution of the edge-mode operator onto a Krylov basis where the dynamics is equivalent to a single particle on a tight-binding lattice with inhomogeneous couplings [20–22]. We find that this lattice for the edge-mode operators is neither that of an operator of a free or integrable model nor is it the lattice typical of a chaotic operator. We give arguments for the general structure of the Krylov lattice of these topological edge modes and analytically extract the lifetime.

Model.—We study the anisotropic XY model of chain length L , perturbed by a transverse field, and by exchange interactions in the z direction,

$$\begin{aligned}
 H &= \sum_{i=1}^L \left[J \left(\frac{1+\gamma}{2} \right) \sigma_i^x \sigma_{i+1}^x + J \left(\frac{1-\gamma}{2} \right) \sigma_i^y \sigma_{i+1}^y \right. \\
 &\quad \left. + J_z \sigma_i^z \sigma_{i+1}^z + g \sigma_i^z \right] \\
 &= H_{XX} + H_{YY} + H_{ZZ} + H_Z,
 \end{aligned} \tag{1}$$

where g and γ denote the strength of the transverse field and the XY anisotropy respectively. We set $J = \hbar = 1$.

A nonzero J_z prevents a mapping to free Jordan-Wigner fermions. The model has a Z_2 symmetry $D_z = \sigma_1^z \sigma_2^z \dots \sigma_L^z$. For $\gamma \neq 0$, $J_z = 0$, $|g| < 1$ or $\gamma \neq 0$, $J_z \neq 0$, $g = 0$ the model supports a strong mode (SM) operator defined as [10,23–26]

$$\{\Psi_0, D_z\} = 0, \quad [H, \Psi_0] \approx u^L; \|u\| < 1. \quad (2)$$

Thus, as $L \rightarrow \infty$, $[H, \Psi_0] = 0$. The existence of an SM implies that the two different parity sectors are degenerate as $L \rightarrow \infty$ [27,28].

When $J_z \neq 0$, the SM turns into an almost strong mode (ASM) [5] that anticommutes with parity but only approximately commutes with H when $L \rightarrow \infty$. For small system sizes, the ASM behaves like the SM as its lifetime increases exponentially with L . For larger L however, its lifetime saturates to a system size independent value.

SM for $J_z = 0$.—While the SM is $\Psi_0 = \sigma_1^x$ when $J_z = g = 0$, $\gamma = 1$, for other parameters, it is a more complicated operator that nevertheless has a finite overlap with σ_1^x . In terms of Majorana fermions, defined as

$$a_{2l-1} = \sigma_l^x \prod_{j=1}^{l-1} \sigma_j^z, \quad a_{2l} = \sigma_l^y \prod_{j=1}^{l-1} \sigma_j^z, \quad (3)$$

and for $\gamma > 0$, we find that the SM localized at one end is [29]

$$\Psi_0 = \sum_{l=1}^{L-1} C_l a_{2l-1}; \quad C_l = \frac{(1+\gamma)/2}{\sqrt{g^2 + \gamma^2 - 1}} (q_+^l - q_-^l),$$

$$q_{\pm} = \frac{g \pm \sqrt{g^2 + \gamma^2 - 1}}{1 + \gamma}. \quad (4)$$

Ψ_0 is normalizable for $g^2 < 1$, $\gamma \neq 0$, indicating that it is localized at the boundary. When $\gamma = 1$, the SM is the familiar one for the Kitaev chain with [10] $C_l = g^{l-1}$. Note that, just like the correlations [30], the spatial character of the SM changes at $g^2 + \gamma^2 = 1$.

Autocorrelation function.—Because of the overlap with σ_1^x when $\gamma > 0$, the SM and ASM (together denoted by (A) SM) might be detected through the infinite temperature autocorrelation function [5] defined as

$$A_{\infty}(t) = \frac{1}{2^L} \text{tr}[\sigma_1^x(t) \sigma_1^x(0)]. \quad (5)$$

Here $\hat{O}(t) = e^{iHt} \hat{O} e^{-iHt}$ denotes Heisenberg time evolution. In general, $A_{\infty}(t) \sim e^{-\Gamma t}$ decays in time. For a finite wire, the (A)SM can tunnel across, and the decay rate is exponentially dependent on L , as suggested in Eq. (2), with $\Gamma \sim e^{-Lh(\gamma, g, J_z)}$ for some function h to be determined. The exponential increase in lifetime with system size is a characteristic of the SM. In contrast, for the ASM, the

exponential increase of lifetime with system size eventually saturates to an L independent result. For example, when $\gamma = 1$, ED suggests a highly nonperturbative dependence $\Gamma \sim e^{-cJ/J_z}$, $c = O(1)$ up to logarithmic corrections [6]. This form is also argued from setting operator bounds on approximately conserved quantities in the prethermal regime [31]. However, a treatment that directly studies the lifetime of topological edge modes and is valid for broader regimes that are not necessarily related to prethermalization is needed.

Lifetime for small system sizes.—We now show that the lifetime for small system sizes is largely governed by perturbative processes. Denoting $|\epsilon_n\rangle$ as an eigenstate of H and parity, even in the presence of integrability breaking terms, $\sigma_1^x |\epsilon_n\rangle \sim |\epsilon'_n\rangle$, where ϵ'_n is the opposite parity energy level nearly degenerate to ϵ_n . Defining $\Delta_n = \epsilon_n - \epsilon'_n$, we find that, to a good approximation, the finite-size behavior is mimicked by [29] $A_{\infty}(t) \sim \sum_n \cos(\Delta_n t) / 2^{L-1}$. For the finite-size decay rate, a perturbative estimate of Δ_n suffices. Below we treat $J_{y,z}$, $g \ll 1$, where $J_y = (1 - \gamma)/2$. Focusing on the two degenerate ground states of H_{XX} (not necessarily of definite parity), we determine the process that gaps the states and from that construct the two gapped states of definite parity. The same considerations hold for every excited level of H_{XX} .

Denoting the eigenstate of σ^x as $\sigma^x |\pm\rangle = \pm |\pm\rangle$, let us first consider the case when g is dominant. L applications of g are required for a transition from one ground state to another, $|++ \dots +\rangle \xrightarrow{(g \sum_i \sigma_i^z)^L} |-- \dots -\rangle$. Thus, the splitting between the ground state sectors is g^L , and the same splitting appears when rotated to the basis of definite parity, $|++ \dots +\rangle \pm |-- \dots -\rangle$. The energy splitting gives a decay rate of the ASM, $\Gamma \sim g^L = e^{\log(g)L}$.

When J_z is the dominant term, the ground state degeneracy is lifted by $L/2$ applications of J_z , $|++ \dots +\rangle \xrightarrow{(J_z \sum_i \sigma_i^z \sigma_{i+1}^z)^{L/2}} |-- \dots -\rangle$, giving an energy splitting and consequently a decay rate $\Gamma \sim (J_z)^{L/2} = e^{\log(J_z)L/2}$. Similar arguments can be applied when J_y is dominant. Since, $\sigma_i^y \sigma_{i+1}^y = -\sigma_i^x \sigma_{i+1}^x \sigma_i^z \sigma_{i+1}^z$, up to an overall sign, J_y is similar to the J_z perturbation and gives $\Gamma \sim (J_y)^{L/2} = e^{\log(J_y)L/2}$. Figure 1 plots Γ obtained from ED. The solid lines are the estimates for Γ from perturbation theory, and they excellently describe the asymptotic behavior of the data. In addition, the plot shows an interesting phenomenon when competing terms affect the lifetime. In particular, when $J_y \sim J_z$, since matrix elements of the two terms have opposite signs, destructive interference between these two scattering channels leads to an enhanced lifetime. This is visible as a pronounced cusp in Fig. 1 when $J_y \sim J_z$.

Krylov basis.—We now discuss the lifetime of the ASM in the system size independent limit. We study the operator dynamics following a Lanczos scheme designed to map the Heisenberg time evolution to a tight-binding model in

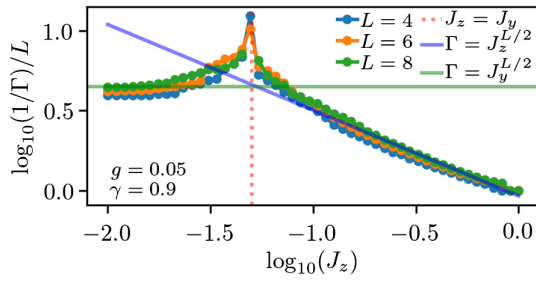


FIG. 1. Decay rate of A_∞ obtained from ED for different L and J_z behaves as $\Gamma = [\max(J_z, J_y)]^{L/2}$, where $g \ll J_{z,y} \ll 1$. When $J_z = J_y$, destructive interference between two scattering channels leads to a pronounced increase of the lifetime, as indicated by the cusp.

Krylov space [20,21]. Note that $\sigma_1^x(t) = e^{iHt}\sigma_1^x e^{-iHt} = \sum_{n=0}^{\infty} [(it)^n/n!] \mathcal{L}^n \sigma_1^x$, where $\mathcal{L} = [H, \cdot]$. We define $\hat{O} = |O\rangle$, and $(O_1|O_2) = (1/2^L)\text{tr}[O_1^\dagger O_2]$. Thus, $A_\infty(t)$ becomes

$$A_\infty(t) = (\sigma_1^x | e^{it\mathcal{L}} | \sigma_1^x). \quad (6)$$

The Pauli basis is 2^{2L} dimensional; hence determining \mathcal{L} outright is generally not feasible. σ_1^x is a Majorana, and when the system is free, the time evolution can only mix with a total of $2L$ Majoranas, and only in this case can \mathcal{L} be completely determined. However, the key observation is that for both free and interacting cases, there is a special basis, the Krylov basis, where \mathcal{L} is tridiagonal and the dynamics of any operator can be mapped to a tight-binding model.

To construct the Krylov basis for, say, σ_1^x , we start with $|O_0\rangle = |\sigma_1^x\rangle$ and construct $|A_1\rangle = \mathcal{L}|O_0\rangle$, $b_1 = \sqrt{\langle A_1|A_1\rangle}$, and $|O_1\rangle = |A_1\rangle/b_1$. These steps are repeated as follows:

$$\begin{aligned} |A_n\rangle &= \mathcal{L}|O_{n-1}\rangle - b_{n-1}|O_{n-2}\rangle, \\ b_n &= \sqrt{\langle A_n|A_n\rangle}; |O_n\rangle = \frac{1}{b_n}|A_n\rangle. \end{aligned} \quad (7)$$

In the Krylov basis, the Liouvillian takes the form

$$\mathcal{L} = H_K = \sum_i b_i (c_i^\dagger c_{i+1} + \text{H.c.}), \quad (8)$$

where c_i^\dagger, c_i are the creation, annihilation operators in the Krylov basis. Recently, this approach has been mainly used to identify chaos [21,22,32]. Below we show that this method is very helpful for studying long-lived topological edge modes.

Lifetime in the thermodynamic limit.—The (A)SM can be constructed by noticing that

$$\begin{aligned} [H_K, c_1^\dagger] &= b_1 c_2^\dagger, & \left[H_K, c_1^\dagger - \frac{b_1}{b_2} c_3^\dagger \right] &= -\frac{b_1 b_3}{b_2} c_4^\dagger, \\ \left[H_K, c_1^\dagger - \frac{b_1}{b_2} c_3^\dagger + \frac{b_1 b_3}{b_2 b_4} c_5^\dagger \right] &= \frac{b_1 b_3 b_5}{b_2 b_4} c_6^\dagger \dots \end{aligned} \quad (9)$$

Thus, the ASM after N iterations is

$$\Psi_0(N) = \sum_{n=0}^N (-1)^n \frac{b_1 b_3 \dots b_{2n-1}}{b_2 b_4 \dots b_{2n}} c_{2n+1}^\dagger. \quad (10)$$

The error, defined by how much $\Psi_0(N)$ does not commute with H_K , is

$$\begin{aligned} \text{error}(N) &= [H, \Psi_0(N)] \\ &= (-1)^N \frac{b_1 \dots b_{2N-1} b_{2N+1}}{b_2 \dots b_{2N}} c_{2N+2}^\dagger. \end{aligned} \quad (11)$$

The error is an important quantity for identifying an (A)SM. This is because for an SM, the error only decreases with subsequent iterations, whereas for an ASM, the error decreases up to a certain N^* and then begins to grow. In addition, as we show below, the error at N^* can be used to determine the lifetime in the thermodynamic limit.

First consider $J_z = 0$, $g^2 < 1$, for which an SM exists [cf. Eq. (4)]. We find that the Krylov Hamiltonian for σ_1^x with $\gamma = 1$ is $b_{\text{odd}} = 2g$, $b_{\text{even}} = 2$ and therefore has a staggered or dimerized structure quantified by $b_{2n} - b_{2n+1} > 0$. For $\gamma \neq 1$, the b_n are shown in Fig. 2 and show a similar staggered structure. Thus, the effective Hamiltonian in the Krylov basis is the Su-Schrieffer-Heeger (SSH) model [33,34], with the SM being the edge mode of the SSH model. For the same parameters, other Pauli operators such as $\sigma_1^{y,z}$ that are not localized at the edge under Heisenberg time evolution have a qualitatively different Krylov Hamiltonian. In particular, σ_1^y is given by an SSH-type model but with a dimerization of the opposite sign to that of σ_1^x , so that the effective Hamiltonian for σ_1^y is topologically trivial and supports no localized edge mode. Since topological protection is robust to moderate disorder, local fluctuations of the above staggered structure in Krylov space will not affect the stability of the edge mode. The pattern of staggering of b_n in Fig. 2 continues until $n \sim O(L)$, after which finite-size effects such as the hybridization of the Majoranas at the ends of the chain set in.

The Krylov basis for σ_1^z is different from $\sigma_1^{x,y}$ in that, to start with, near site 1 the dimerization is negative, corresponding to a topologically trivial phase. But on moving toward the bulk, the average hopping first increases and then plateaus. The net effect on the dynamics is similar to that on σ_1^y in that this lattice causes the operator to spread rapidly into the bulk under time evolution. The lower panel of Fig. 2 shows the A_∞ of the three Pauli operators, with $\sigma_1^{y,z}$ decaying rapidly.

In Fig. 3, the top panel shows how the b_n change on increasing J_z . The corresponding A_∞ is plotted in the lower panel of Fig. 3. One finds that the effect of J_z is twofold. One is to increase the average hopping into the bulk, which appears as a nonzero slope of b_n when plotted against n .

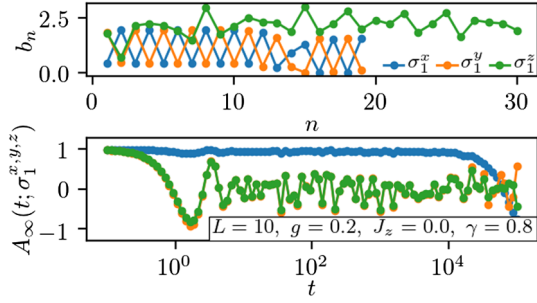


FIG. 2. Top panel: The b_n for the Pauli spins on the first site $\sigma_1^{x,y,z}$ for $J_z = 0$, $\gamma > 0$. The model maps to free fermions and supports an SM with overlap with σ_1^x . The deviation from perfect staggered behavior for $n > 10$ is a finite-size effect. Bottom panel: A_∞ from ED for $\sigma_1^{x,y,z}$. Because of overlap with the SM, σ_1^x persists up to $t \sim 10^4$ as opposed to $\sigma_1^{y,z}$ that decay by $t = O(1)$.

The second effect is to reduce the dimerization with increasing n . Eventually, deep in the bulk, the dimerization vanishes, and the effective hopping increases linearly with position, a behavior expected for a generic chaotic operator [21,22]. The long lifetime of the ASM is entirely due to this crossover from the topologically nontrivial SSH model at small n to chaotic linear couplings at large n .

Effective model in Krylov basis.—We make this more quantitative by adopting the following model for the hopping parameters:

$$\begin{aligned} b_{2n} &= \alpha_0 + \rho\alpha 2n + \delta; & 0 < \alpha \ll \alpha_0 \sim \delta; \\ b_{2n+1} &= \alpha_0 + \alpha(2n + 1); & 0 < 1 - \rho \ll 1. \end{aligned} \quad (12)$$

The even sites have slope $\rho\alpha$, while the odd sites have slope α . At some point the dimerization $b_{2n} - b_{2n+1}$ changes sign as $\rho < 1$. This means that Eq. (11) eventually grows with N and the mode is non-normalizable. We also imposed $1 - \rho \ll 1$ to simplify analytic expressions, but this restriction is not essential.

We can estimate the decay rate from Eq. (11) by finding N^* such that $b_{2N^*+1} = b_{2N^*}$, which gives $N^* \sim \delta/2\alpha(1 - \rho) \gg 1$ and

$$\begin{aligned} \Gamma \sim |\text{error}(N^*)| &= b_1 \exp \left[\sum_{n=1}^{N^*} \ln \left(\frac{b_{2n+1}}{b_{2n}} \right) \right] \\ &\sim \exp \left[-\frac{\delta}{2\alpha} \log \left(\frac{1}{1 - \rho} \right) \right]. \end{aligned} \quad (13)$$

Note that when $\rho = 1$, $\alpha \neq 0$, we still have an SM despite the fact that the b_n have a linear slope $b_n \sim an$. Thus, it is the dimerization, which is preserved when $\rho = 1$, that prevents the operator from spreading. Equation (13) shows that the lifetime depends on J_z nonperturbatively as the slope $\alpha \propto J_z$. We later give numerical and qualitative arguments for this form of the slope.

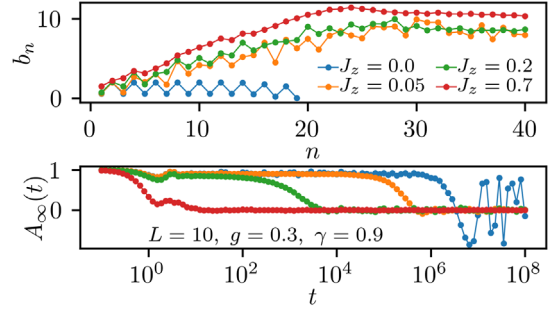


FIG. 3. Top panel: The b_n for increasing J_z with finite-size effects appearing as a plateau for $n > 20$. As L is increased [29], the linear ramp is extended, with the b_n plateauing at a larger n and at a larger value. Bottom panel: A_∞ shows rapid decrease in lifetime with increasing J_z .

It is illuminating to consider the continuum limit of the effective Hamiltonian in the Krylov basis, where the eigenvalue problem may be recast as [29] $E\Psi_n = [(b_{2n-1} - b_{2n} - b_{2n}\partial_n)\sigma^- + \text{H.c.}]\Psi_n$. The edge mode solution is

$$\Psi_{0,n} = e^{-\int_1^n dm(b_{2m} - b_{2m-1})/b_{2m}} \begin{pmatrix} 1 \\ 0 \end{pmatrix}, \quad (14)$$

and shows that the ASM, indeed, decreases in amplitude into the bulk when $(b_{2m} - b_{2m-1})/b_{2m} > 0$. Using the minimal model in Eq. (12), we see that, at N^* , $b_{2N^*} - b_{2N^*+1} = 0$, Eq. (14) stops decreasing with n and mixes with other modes. The decay rate is estimated by the value of ASM at $n = N^*$, $\Gamma \sim \exp[-\int^{N^*} dm(b_{2m} - b_{2m-1})/b_{2m}]$, which recovers Eq. (13).

Comparison of ED with Krylov Hamiltonian with a metallic bulk.—We extract the nonerturbative lifetime using two different numerical methods. The top panel of Fig. 4 compares A_∞ from ED for $L = 14$ to that obtained from time evolving by the Krylov Hamiltonian $\langle n = 1 | [\exp(iH_K t)] | n = 1 \rangle$, where $|n = 1\rangle$ is a state localized at site 1 in the Krylov basis. Since the calculation of the b_n is exponentially expensive in computer resources, only the first ~ 40 b_n are evaluated. Guided by Fig. 3, we simulate a semi-infinite lattice in Krylov space by setting $b_{40 < n < 2e5} = b_{40}$, essentially attaching a metallic reservoir to our inhomogeneous SSH model. The lifetime obtained by both these methods is shown in the lower panel of Fig. 4 and suggests the L independent form $\ln \Gamma \propto -1/J_z$. Thus, for the purpose of capturing the lifetime, the simple model for the bulk b_n is an efficient alternative to ED. In addition, the saturation of the lifetime implies that it is controlled by the dimerization of the b_n at small and intermediate n [29].

Qualitative argument for $\alpha \propto J_z$.—We supplement the above results for the decay rate by a qualitative argument for $\alpha \propto J_z$. For simplicity we restore J and consider $\gamma = 1$. When $J_z = g = 0$, then $H = H_{XX} = JN$ counts the number of domain walls $N = \sum_i \sigma_i^x \sigma_{i+1}^x$. When $J_z \neq 0$ we

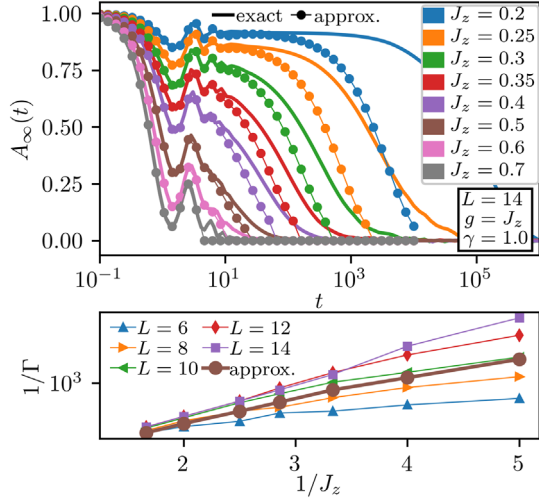


FIG. 4. Top panel: A_∞ from ED for $L = 14$, with $J_z = g$ increasing from the top to the bottom of the panel. It is compared with the approximate A_∞ obtained from time evolution in a Krylov basis with ~ 40 exact b_n [29] and $b_{40 < n < n_{\max}} = b_{40}$ held constant, mimicking a reservoir. We choose $n_{\max} = 2e5$, which is large enough to capture the decay of the ASM before finite-size effects set in. Bottom panel: Decay rate extracted from both numerical methods. For $1/J_z < 4$, the overlapping lines for $L = 12, 14$ indicate saturation of the lifetime.

recast $H_{ZZ} = J_z D + J_z \tilde{E}$, where D commutes with N , whereas \tilde{E} does not. We find that the operator

$$D = \sum_j P_j \sigma_j^z \sigma_{j+1}^z; \quad P_j = \frac{1}{2} [1 - \sigma_{j-1}^x \sigma_j^x \sigma_{j+1}^x \sigma_{j+2}^x], \quad (15)$$

does not change the number of domain walls and commutes with N [29]. D is essentially a hopping term for domain walls. In the basis that simultaneously diagonalizes D , N , we find that the minimal energy to create a domain wall in the bulk is reduced from $2J$ to $2J - J_z$ and that domain wall particle-hole pairs have energies of $O(J_z)$. Now consider $J_z \ll g$. Then the leading term noncommuting with N is H_Z .

As argued for a different model [7], the energy cost for flipping a spin at the edge is $\sim J$. Thus, a creation of $\sim J/J_z$ pairs of domain walls in the bulk can offset the energy J required to flip an edge spin. This requires J/J_z applications of the transverse field g . Therefore the Fermi golden rule estimate for the decay rate is

$$\Gamma \sim g \left[\frac{g}{J} \right]^{cJ/J_z}, \quad c = O(1). \quad (16)$$

Up to logarithms, this decay rate is consistent with ED [6] (Fig. 4), operator bounds in the prethermal regime [31], and time evolution using a truncated Krylov Hamiltonian (Fig. 4).

Summary.—We have presented a new way to extract the nonperturbatively long lifetimes of ASMs. We showed that the Krylov Hamiltonian for the ASM has linearly growing hopping along with decreasing dimerization, where the dimerization is associated with the existence of the ASM and is key to preventing chaotic operator growth. Essentially the operator dynamics is that of a particle that is trapped for a long time as a quasistable SSH edge mode that eventually escapes via tunneling. We demonstrated that a truncated Krylov Hamiltonian terminating in a metallic bulk is an efficient way for capturing the lifetime of the ASM. We also found that competing terms can interfere to enhance the lifetime (Fig. 1). It would be interesting to identify additional structures of the Krylov Hamiltonian, besides dimerization, that can support long-lived edge modes. More broadly, generalization of this study to other topological states, both static and Floquet, and in any spatial dimension is an exciting avenue for future research.

This work was supported by the U.S. Department of Energy, Office of Science, Basic Energy Sciences, under Award No. DE-SC0010821 (D. J. Y. and A. M.) and by the U.S. National Science Foundation Grant No. NSF DMR-1606591 (A. G. A.).

- [1] D. J. Thouless, M. Kohmoto, M. P. Nightingale, and M. den Nijs, *Phys. Rev. Lett.* **49**, 405 (1982).
- [2] J. Bellissard, A. van Elst, and H. Schulz Baldes, *J. Math. Phys. (N.Y.)* **35**, 5373 (1994).
- [3] X.-L. Qi and S.-C. Zhang, *Rev. Mod. Phys.* **83**, 1057 (2011).
- [4] S. Ryu, A. P. Schnyder, A. Furusaki, and A. W. W. Ludwig, *New J. Phys.* **12**, 065010 (2010).
- [5] J. Kemp, N. Y. Yao, C. R. Laumann, and P. Fendley, *J. Stat. Mech.* **05** (2017) 063105.
- [6] D. V. Else, P. Fendley, J. Kemp, and C. Nayak, *Phys. Rev. X* **7**, 041062 (2017).
- [7] J. Kemp, N. Y. Yao, and C. R. Laumann, [arXiv:1912.05546](https://arxiv.org/abs/1912.05546).
- [8] T. Rakovszky, P. Sala, R. Verresen, M. Knap, and F. Pollmann, *Phys. Rev. B* **101**, 125126 (2020).
- [9] A. Altland and M. R. Zirnbauer, *Phys. Rev. B* **55**, 1142 (1997).
- [10] A. Y. Kitaev, *Phys. Usp.* **44**, 131 (2001).
- [11] A. Kitaev, *Ann. Phys. (Amsterdam)* **321**, 2 (2006), Special Issue.
- [12] L. Fidkowski and A. Kitaev, *Phys. Rev. B* **83**, 075103 (2011).
- [13] C. Nayak, S. H. Simon, A. Stern, M. Freedman, and S. Das Sarma, *Rev. Mod. Phys.* **80**, 1083 (2008).
- [14] P. Fendley, M. P. Fisher, and C. Nayak, *Ann. Phys. (Amsterdam)* **324**, 1547 (2009).
- [15] J. Alicea, *Rep. Prog. Phys.* **75**, 076501 (2012).
- [16] C. Beenakker, *Annu. Rev. Condens. Matter Phys.* **4**, 113 (2013).
- [17] D. E. Parker, R. Vasseur, and T. Scaffidi, *Phys. Rev. Lett.* **122**, 240605 (2019).
- [18] L. M. Vasiloiu, F. Carollo, and J. P. Garrahan, *Phys. Rev. B* **98**, 094308 (2018).

- [19] D. J. Yates, F. H. L. Essler, and A. Mitra, *Phys. Rev. B* **99**, 205419 (2019).
- [20] V. Vishwanath and G. Müller, *The Recursion Method: Applications to Many-Body Dynamics* (Springer, New York, 2008).
- [21] D. E. Parker, X. Cao, A. Avdoshkin, T. Scaffidi, and E. Altman, *Phys. Rev. X* **9**, 041017 (2019).
- [22] J. Barbón, E. Rabinovici, R. Shir, and R. Sinha, *J. High Energy Phys.* **10** (2019) 264.
- [23] P. Fendley, *J. Stat. Mech.* **11** (2012) P11020.
- [24] A. S. Jermyn, R. S. K. Mong, J. Alicea, and P. Fendley, *Phys. Rev. B* **90**, 165106 (2014).
- [25] P. Fendley, *J. Phys. A* **49**, 30LT01 (2016).
- [26] I. A. Maceira and F. Mila, *Phys. Rev. B* **97**, 064424 (2018).
- [27] N. Moran, D. Pellegrino, J. K. Slingerland, and G. Kells, *Phys. Rev. B* **95**, 235127 (2017).
- [28] L. M. Vasiloiu, F. Carollo, M. Marcuzzi, and J. P. Garrahan, *Phys. Rev. B* **100**, 024309 (2019).
- [29] See Supplemental Material at <http://link.aps.org/supplemental/10.1103/PhysRevLett.124.206803> for 3 supplementary plots for the autocorrelation function and the b_n , derivation of SM for general γ , derivation of the continuum model, and derivation of Eq. (16).
- [30] F. Franchini and A. G. Abanov, *J. Phys. A* **38**, 5069 (2005).
- [31] D. Abanin, W. De Roeck, W. W. Ho, and F. Huveneers, *Commun. Math. Phys.* **354**, 809 (2017).
- [32] A. Dymarsky and A. Gorsky, [arXiv:1912.12227](https://arxiv.org/abs/1912.12227).
- [33] W. P. Su, J. R. Schrieffer, and A. J. Heeger, *Phys. Rev. Lett.* **42**, 1698 (1979).
- [34] W. P. Su, J. R. Schrieffer, and A. J. Heeger, *Phys. Rev. B* **22**, 2099 (1980).